Adaptive Integral Method for Higher-Order Hierarchical Method of Moments

Kim, Oleksiy S.; Meincke, Peter

Published in:
Proceedings of the European Conference on Antennas and Propagation EuCAP 2006

Link to article, DOI:
10.1109/EUCAP.2006.4584498

Publication date:
2006

Document Version
Publisher's PDF, also known as Version of record

ADAPTIVE INTEGRAL METHOD FOR HIGHER-ORDER HIERARCHICAL METHOD OF MOMENTS

O. S. Kim and P. Meincke

Ørsted•DTU, Electromagnetic Systems, Technical University of Denmark,
Ørsteds Plads, Building 348, DK-2800 Kgs. Lyngby, Denmark
Email: osk@oersted.dtu.dk

ABSTRACT

The Adaptive Integral Method (AIM) is applied to solve the volume integral equation in conjunction with the higher-order Method of Moments (MoM). The classical AIM is modified for larger discretization cells to take advantage of higher-order MoM. The technique combines the low computational complexity and memory requirements of AIM with the reduced number of unknowns and higher-order convergence of higher-order hierarchical Legendre basis functions. Numerical examples given show the advantages of the proposed technique over AIM based on low-order basis functions in terms of memory and computational time. Several preconditioning techniques applied to AIM for volume integral equations are considered.

Key words: scattering, adaptive integral method (AIM), volume integral equation, method of moments, higher-order hierarchical Legendre basis functions.

1. INTRODUCTION

Integral equations applied to scattering problems for arbitrarily shaped inhomogeneous dielectric objects are usually solved with the Method of Moments (MoM). This procedure leads to a dense system of linear equations with the memory requirement $O(N^2)$ and solution complexity $O(N^3)$ for a direct solver and $O(N^2)$ for an iterative one, with N being the number of unknowns. It is evident that computational demands increase drastically as the problem size grows. In the case of compact penetrable volumetric scatterers, practically available computer resources limit the scatterer size to an order of one wavelength.

Fast integral equation solvers, such as the Multilevel Fast Multiple Method (MLFMM) or the Adaptive Integral Method (AIM), reach the solution complexity of $O(N \log N)$ and are able to reduce the memory demands for volumetric problems to the order of $O(N \log N)$ and $O(N)$, respectively. Alternatively, higher-order hierarchical basis functions can be employed in the conventional MoM to significantly reduce the number of unknowns, which in many practical cases is more memory and computationally efficient as compared to the fast solvers based on low-order basis functions (RWG, rooftop, or pulse) [1]. The obvious step further is to use the fast solvers with higher-order basis functions. In [2], MLFMM is applied to surface integral equations discretized with higher-order interpolatory basis functions. The computational complexity and memory requirements of this technique are addressed in [3].

In this paper, AIM is employed to accelerate the solution of the volume integral equation (VIE) with higher-order hierarchical basis functions. The usage of the higher-order basis functions becomes advantageous when they are defined in relatively large cells, which contradicts with accuracy conditions for expansions established in AIM [4]. To preserve low computational complexity and memory requirements of AIM the appropriate modifications are developed. Among various types of higher-order hierarchical basis functions a set of basis functions based on the orthogonal Legendre polynomials are chosen [5] due to their favorable properties with respect to the iterative solver convergence [6]. Numerical examples for a dielectric sphere and cube are given to validate the presented technique as well as to show its efficiency.

2. FORMULATION

2.1. Higher-order MoM for VIE

The VIE is based on the volume equivalence principle and expresses the total electric field in the volume V in terms of the free-space Green's function $G(\mathbf{r}, \mathbf{r}')$ and the unknown induced volume current density $\mathbf{J}(\mathbf{r})$ due to the incident field $\mathbf{E}^{\mathrm{i}}(\mathbf{r})$ as

$$\mathbf{E}^{\mathrm{i}}(\mathbf{r}) = \frac{\mathbf{D}(\mathbf{r})}{\varepsilon(\mathbf{r})} + j\omega\mu_0 \int_V G(\mathbf{r}, \mathbf{r}')\mathbf{J}(\mathbf{r}')dV' + \nabla\Phi, \quad (1)$$

Proc. 'EuCAP 2006', Nice, France
6–10 November 2006 (ESA SP-626, October 2006)

where $\mathbf{D}(\mathbf{r})$ is the electric flux density, and

$$\Phi(\mathbf{r}) = \frac{j\omega\mu_0}{k_0^2}\int_V G(\mathbf{r},\mathbf{r}')[\nabla'\cdot\mathbf{J}(\mathbf{r}')]dV' - \frac{j\omega\mu_0}{k_0^2}\int_S G(\mathbf{r},\mathbf{r}')\big[\mathbf{J}(\mathbf{r})\cdot\mathbf{dS}'\big]. \quad (2)$$

In Eq.2, k_0 is the wavenumber in free space and S is the surface enclosing the volume V. The VIE (Eq.1) is more conveniently solved with respect to the electric flux density $\mathbf{D}(\mathbf{r})$ rather than the induced current density $\mathbf{J}(\mathbf{r})$, since the normal component of $\mathbf{D}(\mathbf{r})$ is continuous across the boundary between two different dielectric materials. This change in variables is carried out by the substitution

$$\mathbf{J}(\mathbf{r}) = j\omega\frac{\varepsilon(\mathbf{r})-\varepsilon_0}{\varepsilon(\mathbf{r})}\mathbf{D}(\mathbf{r}). \quad (3)$$

The higher-order MoM is applied to transform the VIE into a system of linear equations. The process involves the discretization of the object with higher-order curvilinear hexahedral elements and expansion of the electric flux density $\mathbf{D}(\mathbf{r})$ in each element in terms of the higher-order hierarchical Legendre basis functions [5] as

$$D^{\xi} = \frac{1}{A}\sum_{m=0}^{M^{\xi}}\sum_{n=0}^{N^{\zeta}}\sum_{q=0}^{Q^{\eta}} a^{\xi}_{mnq}\tilde{P}_m(\xi)P_n(\zeta)P_q(\eta), \quad (4)$$

where (ξ,ζ,η) is (u,v,w), (v,w,u), or (w,u,v), A is the Jacobian of the parametric transformation, a^{ξ}_{mnq} are unknown coefficients, and M^{ξ}, N^{ζ}, and Q^{η} denote the expansion orders. The function $\tilde{P}_m(\xi)$ is defined as

$$\tilde{P}_m(\xi) = \begin{cases} 1-\xi, & m=0 \\ 1+\xi, & m=1 \\ P_m(\xi)-P_{m-2}(\xi), & m\geq 2, \end{cases} \quad (5)$$

where $P_m(\xi)$ are Legendre polynomials. Morevover, (u,v,w) denote the local curvilinear coordinate system of each element, which is mapped to the physical space by the Lagrange interpolation.

2.2. Adaptive Integral Method for higher-order MoM

The main idea behind AIM is to split the MoM matrix in two parts, responsible for nearby and far interactions, as $Z = Z^{\text{near}} + Z^{\text{far}}$. Only elements of Z^{near} are computed and stored explicitly. To account for the far interactions, the object is placed in a regular rectangular grid with the step size a (Fig. 1), and the basis functions $\psi_\alpha(\mathbf{r})$ are expanded in terms of Dirac delta functions defined at nodes of this grid as [4]

$$\psi_\alpha(\mathbf{r}) \simeq \sum_{\mathbf{u}\in C_\alpha}\Lambda_{\alpha\mathbf{u}}\delta(\mathbf{r}-\mathbf{u}), \quad (6)$$

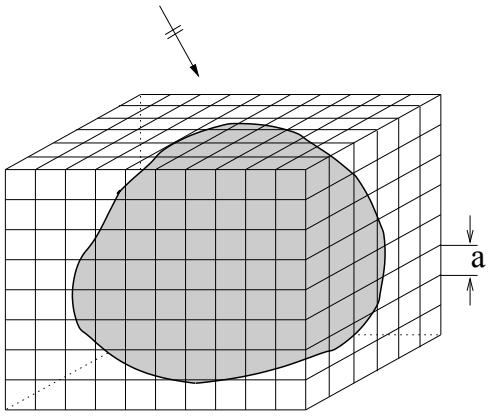

Figure 1. Auxiliary rectangular grid for the far interaction computations in AIM.

where C_α is a cube of $(L+1)^3$ nodes. Then, the computation of the matrix-vector product $Z^{\text{far}}X$, with X denoting the unknown solution vector, at each iteration of the iterative solution process is sped up by application of the FFT. The accuracy of the expansion in Eq. 6 is controlled by the expansion order L, the support size b of the basis function, and the grid step size a. To assure a reasonable error both k_0a and k_0b should satisfy the relation [4]

$$\frac{(\max\{b,La\}k_0)^{L+1}}{(L+1)!} \ll 1 \quad (7)$$

More precise error estimates can be found in [4].

In the case of low-order basis functions, for which AIM was first developed, $\psi_\alpha(\mathbf{r})$ is assumed to span two neighbor cells, so that $\psi_\alpha(\mathbf{r}) = \psi^+_\alpha(\mathbf{r}) + \psi^-_\alpha(\mathbf{r})$. Thus, the support b is the sum of the corresponding cell sizes. The usage of the higher-order basis functions becomes advantageous when they are defined in relatively large cells, allowing high expansion orders. However, a large support size b contradicts the accuracy condition (Eq. 7). To alleviate this we expand the two parts of the rooftop basis functions (first- and higher-order) separately in each cell as

$$\begin{aligned}\psi_\alpha(\mathbf{r}) &= \psi^+_\alpha(\mathbf{r}) \quad + \quad \psi^-_\alpha(\mathbf{r}) \\ &\simeq \sum_{\mathbf{u}\in C^+_\alpha}\Lambda^+_{\alpha\mathbf{u}}\delta(\mathbf{r}-\mathbf{u}) \quad + \quad \sum_{\mathbf{u}\in C^-_\alpha}\Lambda^-_{\alpha\mathbf{u}}\delta(\mathbf{r}-\mathbf{u}). \quad (8)\end{aligned}$$

Hence, we effectively reduce the support b in the expansion to the size of a single cell, which implies that larger cells with higher expansion orders can be utilized. Moreover, the modified expansion allows uniform treatment of both rooftops defined in two cells and higher-order basis functions defined in one cell.

It should be noted that even though the modified expansion required some extra memory to store two coefficient matrices $\Lambda^+_{\alpha\mathbf{u}}$ and $\Lambda^-_{\alpha\mathbf{u}}$ instead of just one $\Lambda_{\alpha\mathbf{u}}$ in Eq.6, the storage requirement does not double since the second matrix $\Lambda^-_{\alpha\mathbf{u}}$ is used only for rooftop basis functions which span two cells. For higher-order basis functions only $\Lambda^+_{\alpha\mathbf{u}}$ is utilized.

3. NUMERICAL RESULTS AND DISCUSSION

In the following numerical experiments the Generalized Minimal Residual (GMRES) iterative algorithm with restarts after 30 iterations is employed.

The first example involves plane wave scattering by a solid sphere of diameter $1\lambda_0$ made of lossless dielectric with relative permittivity $\varepsilon_r = 4.0$. The sphere is represented by 545 trilinear and curvilinear hexahedral elements, and $M_\xi = 2$ expansion order for the unknown electric flux density is utilized in the solution, resulting in 14100 unknowns. The object is placed in a 52x52x52 AIM auxiliary grid with orders $L = 3$-4 depending one the size of each hexahedral element. With the single precision arithmetic the classical MoM would require 1.5 GB of computer memory to store the full impedance matrix, while for the AIM solution only 350 MB are necessary. Fig. 2 shows excellent agreement between the obtained AIM result and the exact Mie series solution used as a reference.

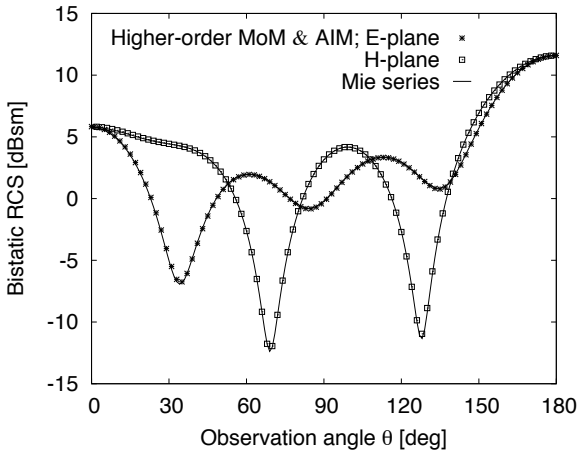

Figure 2. Bistatic RCS of a $1\lambda_0$ dielectric sphere.

In the example above with no preconditioner applied the convergence to a relative residual error of 10^{-5} is achieved with 217 iterations (double precision arithmetic). To improve the convergence rate several preconditioning techniques have been tested. Results for the simplest diagonal Jacobi, inverse-based multilevel incomplete LU (ILU) preconditioner [7], and the complete LU preconditioner are presented in Tab. 1. All preconditioners are computed from the elements of the sparse matrix Z^{near}, since this is the only part of the MoM matrix available explicitly in the AIM technique. The corresponding percentage of non-zero terms in the preconditioner matrix and its fill-in relative to the Z^{near} matrix are also given in Tab. 1. It can be observed that the LU preconditioner provides the best convergence. However, the price paid is a large number of non-zero elements in the preconditioner matrix. A good compromise between the convergence rate and the memory required to store the preconditioner matrix can be achieved with the ILU preconditioner in which the drop tolerance δ is taken as a parameter. For instance, $\delta = 0.05$ is optimal in this case, since further increase of the drop tolerance yields only a little convergence improvement, while the fill-in almost triples. The disadvantage of the employed ILU preconditioner is that the memory required to store the preconditioner matrix is not known in advance.

Table 1. Number of iterations to converge, percentage of non-zero terms in the preconditioner matrix, and its fill-in relative to the Z^{near} matrix. The results are for a dielectric sphere.

Preconditioner	Iterations	Non-zeros,%	Fill-in
Jacobi	173	0.007	0.0004
ILU ($\delta = 0.1$)	128	2.955	0.2005
ILU ($\delta = 0.05$)	73	2.482	0.1684
ILU ($\delta = 0.01$)	61	6.789	0.4606
LU	57	58.558	3.9726

The next example is employed to validate the higher-order convergence of the presented technique. The test object is a dielectric cube ($\varepsilon_r = 4.0$) with side length $1.4\lambda_0$. Mesh sizes from 216 to 42875 hexahedral elements are applied and the expansion order is varied from $M^\xi = 1$ to $M^\xi = 3$. The reference RCS is obtained by the surface integral equation method with the rooftop basis functions ($M^\xi = 1$) on a finely discretized mesh. Fig. 3 shows the root mean square (RMS) error, the computer memory used, and the time spent at each iteration versus the number of unknowns. The double precision arithmetic is utilized in this case. The higher slope of the convergence curves for $M^\xi = 2$ and $M^\xi = 3$ as compared to the $M^\xi = 1$ curve in Fig 3(a) indicates the higher-order convergence of the method. Extrapolation of the $M^\xi = 1$ curve to the RMS error of 0.01 shows that to achieve this accuracy the solution with $M^\xi = 1$ would require at least 2.5 and 4 times more memory than the solution with $M^\xi = 2$ and $M^\xi = 3$, respectively.

In Fig. 3(b) it can be observed that the memory usage increases with the expansion order M^ξ for the same number of unknowns. This is the natural result for the higher-order basis functions, since the number of basis functions defined over the same cell increases with M^ξ, which makes the matrix Z^{near} more populated. However, the result for the computational complexity is not that obvious. As it can be seen in Fig. 3(c) the solutions with $M^\xi = 2$ require less time per iteration than the solutions with $M^\xi = 1$ and $M^\xi = 3$. It can be explained as follows. The most of time spent at each iteration is due to the computation of the matrix-vector product $ZX = Z^{\text{near}}X + Z^{\text{far}}X$, where the first and the second terms are calculated by a standard sparse matrix-vector product and FFT, respectively. As it was stated above, the increase of the expansion order M^ξ results in a more dense Z^{near}, which slows down the computation of the first term in the matrix-vector product ZX. At the same

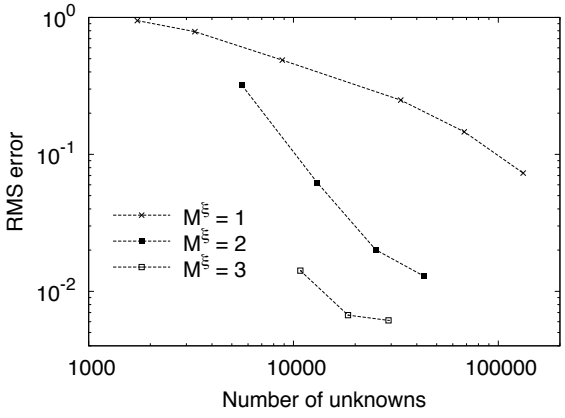

(a)

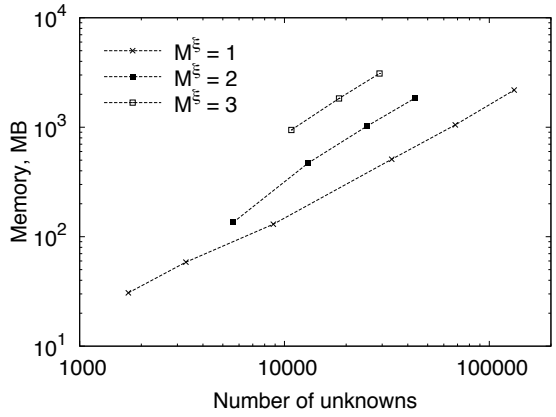

(b)

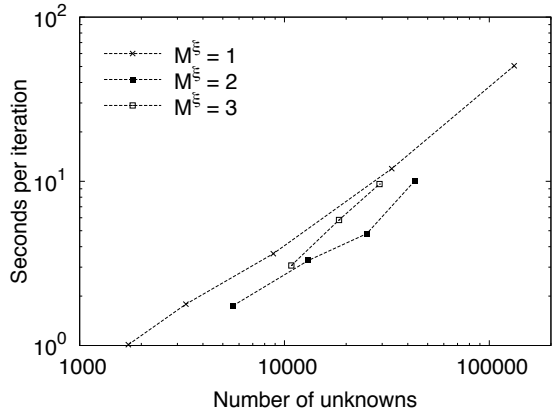

(c)

Figure 3. RMS error, the computer memory used, and the time spent at each iteration versus the number of unknowns. The results are for a dielectric cube.

time, higher-order basis functions are defined in larger cells, which allows a coarser AIM auxiliary grid, and consequently, more fast FFT calculation of the second term in the matrix-vector product ZX. Evidently, for the given example the expansion order $M^{\xi} = 2$ provides the best compromise between the density of Z^{near} and the size of the AIM auxiliary grid.

It should be noted that coarser meshes with cells lager than given in the second example cannot be utilized since the accuracy condition (Eq. 7) is violated. Moreover, further increase of the expansion order M^{ξ} would lead to unreasonable waste of computational resources both in terms of memory and computational time. Therefore, the use of the expansion orders higher than $M^{\xi} = 2$-3 is not desirable.

4. CONCLUSIONS

The solution of the volume integral equation with higher-order MoM is accelerated by the Adaptive Integral Method. Higher-order hierarchical Legendre basis functions and higher-order curvilinear hexahedral elements are employed to discretize the integral equation. The key feature of the presented technique is that the basis functions that span two cells are expanded in AIM separately in each cell, thus allowing larger cells and higher expansion orders to be properly handled. Provided numerical examples illustrate the accuracy and the higher-order convergence of the method. The issues on the computational complexity and the memory requirements are also addressed. It is shown that AIM with higher expansion orders provide better performance than the classical AIM based on low-order basis functions. Among several preconditioning techniques tested the ILU preconditioner tends to be an optimal one in terms of the convergence improvements of the iterative solution process and memory required to store the preconditioner matrix.

REFERENCES

[1] O. S. Kim, P. Meincke, O. Breinbjerg, and E. Jørgensen. *Radio Science*, 39, RS5003, doi:10.1029/2004RS003041, 2004.

[2] K. C. Donepudi, J.-M. Jin, S. Velamparambil, J. Song, and W. C. Chew. *IEEE Trans. Antennas Propagat.*, 49(7):1069–1078, July 2001.

[3] Min Meng, Jun Hu, and ZaiPing Nie. In *Proc. of 3rd Int. Conf. Computational Electromagnetics and Its Applications*, pages 107–110, Nov. 1-4 2004.

[4] E. Bleszynski, M. Bleszynski, and T. Jaroszewicz. *Radio Science*, 31(5):1225–1251, Sept.-Oct. 1996.

[5] E. Jørgensen, J. L. Volakis, P. Meincke, and O. Breinbjerg. *IEEE Trans. on Antennas and Propagation*, 52(11):2985–2995, November 2004.

[6] D. S. Sumic and B. M. Kolundžija. In *Proceedings of the 2005 IEEE Antennas and Propagation Soc. Int. Symp.*, volume 4a, pages 288–291, Washington, DC, July 2005.

[7] Matthias Bollhöfer and Yousef Saad. ILUPACK - preconditioning software package. Available online at http://www.math.tu-berlin.de/ilupack/. Release V1.0, May 14 2004.